Available online at www.sciencedirect.com
ScienceDirect
Fluid Phase Equilibria 261 (2007) 230–237
FLUID PHASE EQUILIBRIA
www.elsevier.com/locate/fluid

Calculation of the interfacial tension of the methane–water system with the linear gradient theory

Kurt A.G. Schmidt [a,*], Georgios K. Folas [b], Bjørn Kvamme [a]

[a] *Department of Physics and Technology, University of Bergen, Allégaten 55, N-5007 Bergen, Norway*
[b] *Center for Phase Equilibria and Separation Processes (IVC-SEP), Technical University of Denmark, Department of Chemical Engineering, Building 229, DK-2800 Lyngby, Denmark*

Received 6 April 2007; received in revised form 11 July 2007; accepted 11 July 2007
Available online 20 July 2007

Abstract

The linear gradient theory (LGT) combined with the Soave–Redlich–Kwong (SRK EoS) and the Peng–Robinson (PR EoS) equations of state has been used to correlate the interfacial tension data of the methane–water system. The pure component influence parameters and the binary interaction coefficient for the mixture influence parameter have been obtained for this system. The model was successfully applied to correlate the interfacial tension data set to within 2.3% for the linear gradient theory and the SRK EoS (LGT-SRK) and 2.5% for the linear gradient theory and PE EoS (LGT-PR). A posteriori comparison of data not used in the parameterisation were to within 3.2% for the LGT-SRK model and 2.7% for the LGT-PR model. An exhaustive literature review resulted in a large database for the investigation which covers a wide range of temperature and pressures. The results support the success of the linear gradient theory modelling approach for this system.

Keywords: Interfacial tension; Methane; Water; Binary mixture; Linear gradient theory; Peng–Robinson; Soave–Redlich–Kwong; Equation of state

1. Introduction

As the world's conventional sources of oil and gases are disappearing, accurate knowledge of the physical properties of these systems is becoming increasingly important. One important, but often overlooked physical property is the interfacial tension between reservoir fluids and water. Accurate determination of this interfacial tension is very important in the exploration, production and processing of petroleum fluids [1–8].

While the interfacial tension of hydrocarbon–water systems is of theoretical and practical interest, there is a paucity of data available in the open literature. If we consider methane, the major component in reservoir fluids, some of the published data sets clearly show discrepancies when compared with each other [3,5–7,9,10]. As such, there is a definite need to collect and evaluate the data for this system and for the other components found in petroleum–water systems.

There are a number of techniques to model the interfacial tension which range from the simple empirical correlations [5,7,11–13] to those based on statistical thermodynamics [14–16]. Unfortunately, the simpler methods, such as the Parachor method, suffer in their accuracy to model the hydrocarbon–water systems [5,7]. The techniques derived from statistical thermodynamics and the theory of inhomogeneous fluids has been shown to be more theoretically sound, accurate and robust calculation method [14–16]. However, due to their complexity, a number of the methods used to calculate interfacial tensions are unsuitable for engineering applications.

Zuo and Stenby developed the linear gradient theory (LGT) [3,17–19], a practical version of the gradient theory [14–16] which eliminates the need to solve the set of time consuming density profile equations that are inherent with the gradient theory approach. This speeds up the calculation procedure without significantly losing accuracy for these types of mixtures.

In this work, the existing experimental methane–water interfacial tension data available in the open literature will be reviewed and modelled with the linear gradient theory combined with the Peng–Robinson (PR EoS) [20] and the Soave–Redlich–Kwong (SRK EoS) [21] equations of state. This will form the basis of a complete database and parameterisation of the linear gradient theory combined with these equations of

* Corresponding author.
E-mail address: kurt.schmidt@ift.uib.no (K.A.G. Schmidt).

0378-3812/$ – see front matter © 2007 Elsevier B.V. All rights reserved.
doi:10.1016/j.fluid.2007.07.045

state for hydrocarbon–water interfacial tension of these components commonly found in reservoir fluids.

2. Literature review

Accurate modelling techniques are data driven and the development of these techniques requires a thorough knowledge of existing literature data. As such, an exhaustive literature review all of the existing experimental methane–water interfacial tension data available in the open literature was performed. The open data were reviewed and used to determine the necessary parameters in the linear gradient theory [3,17–19], combined with the Peng–Robinson equation of state (LGT-PR) and the Soave–Redlich–Kwong equation of state (LGT-SRK). This data compilation greatly expands the temperature and pressure region of the interfacial tension data used by Zuo and Stenby [3] and Yan et al. [22] (Zhao et al. [23]) in their determination of the parameters for the LGT combined with the SRK EoS. In addition, this review assists in identifying where additional data are needed to fill voids and resolve discrepancies of existing data sets.

A complete list of the data sets used in this investigation is presented in Table 1. Overall the collected data set consists of 286 points ranging in temperature from 275.2 to 473.0 K and pressures up to 260 MPa.

The majority of the data was measured at temperatures of 298 K (298–298.2 K), 91 points out of the 286 data points collected were at this temperature.

3. Linear gradient theory model

There are numerous investigations into the use of the gradient theory model combined with an equation of state to determine the interfacial tension of pure component and mixture systems [14–16]. When applied to mixtures the gradient theory requires the solution of time-consuming density profile equations before the interfacial tension can be determined. The numerical effort in resolving the density profiles has been described in detail in the works of Carey [14], Cornelisse [15] and Miqueu [16]. To ease the burden of computational effort, Zuo and Stenby [3,17–19] proposed the linear gradient theory. In the linear gradient theory the density of each component in the mixture is assumed to be distributed linearly between the phases in equilibrium. This assumption eliminates the need to solve the density profile equations found in the gradient theory and speeds up the calculation procedure without significantly losing accuracy for these types of mixtures.

Table 1
Experimental investigations of the interfacial tension of the methane–water system

Investigators	Year	Temperature (K)	Pressure (MPa)
Hocott [24]	1938	298.7–338.7	0.1–24.2
Hough et al. [25]	1951	296.5–410.9	0.1–103.4
Slowinski et al.[a] [26]	1957	298.2	2.1–7.0
Jennings and Newman [27]	1971	296.5–449.8	0.1–82.7
Massoudi and King [28]	1975	298.2	0.01–7.5
Jho et al. [29]	1978	275.2–323.2	0.4–6.6
Wiegand and Franck [30]	1994	298.0–473.0	0.1–240.0
Sachs and Meyn [9]	1995	298.2	0.4–46.9
Tian et al. [31]	1997	298.0–473.0	0.1–100.0
Lepski [32]	1997	325.7–400.0	10.3–24.1
Ren et al. [33]	2000	298.2–373.2	1.0–30.0
Zhao et al. [23]	2002	298.2–373.2	1.0–30.0
Sun et al. [34]	2004	298.2	1.0–30.0

[a] Digitized from the figures (data not tabulated).

According to the linear gradient theory, the molar density (ρ_i) of component i in a mixture is distributed evenly between the co-existing equilibrium bulk phases (e.g. vapour and liquid) through a planar interface of height h. The density of component i at position z in the interface can be represented by:

$$\frac{\mathrm{d}\rho_i(z)}{\mathrm{d}z} = D_i \tag{1}$$

$$D_i = \frac{\Delta\rho_i}{h} = \frac{\rho_i^{\mathrm{II}} - \rho_i^{\mathrm{I}}}{h} \tag{2}$$

where D_i is a constant for each component and ρ_i^{II} and ρ_i^{I} represent the density of component i at the boundary conditions (i.e. the coexisting equilibrium phases). Based on this assumption, the density of each component in the mixture can be determined anywhere along the interface as long as D_i is known. This eliminates the need to solve the inherent density profiles equations in the gradient theory used to determine density $\rho_i(z)$ throughout the interface.

Once the density profile is known, similar to the gradient theory, the interfacial tension is determined with:

$$\gamma = \int_{\rho_1^{\mathrm{I}}}^{\rho_1^{\mathrm{II}}} \sqrt{2c(\Phi(\rho) - \Phi_{\mathrm{B}})}\mathrm{d}\rho_1 \tag{3}$$

where c, $\Phi(\rho)$, Φ_{B} are the mixture influence parameter, grand thermodynamic potential energy density and negative pressure ($-P$). Subscript *1* represents the component (among the *Nc* number of components) with the maximum value of the density difference between the two homogenous phases, i.e.:

$$\Delta\rho_1 = \max(\rho_i^{\mathrm{I}} - \rho_i^{\mathrm{II}}) \qquad i = 1, 2, \ldots \mathrm{Nc} \tag{4}$$

The grand thermodynamic potential energy density is determined from an equation of state via the Helmholtz free energy, $f^0(\rho)$, and chemical potentials of each species, μ_i. The grand thermodynamic potential energy density is defined by:

$$\Phi(\rho) = f^0(\rho) - \sum_{i=1}^{\mathrm{Nc}} \rho_i \mu_i \tag{5}$$

In the linear gradient theory the mixture influence parameter may determined by [3]:

$$c = \sum_{i=1}^{\mathrm{Nc}}\sum_{j=1}^{\mathrm{Nc}} c_{ij} \left(\frac{\Delta\rho_i}{\Delta\rho_1}\right)\left(\frac{\Delta\rho_j}{\Delta\rho_1}\right) \tag{6}$$

or [17]:

$$c = \sum_{i=1}^{Nc}\sum_{j=1}^{Nc} c_{ij}x_i x_j \tag{7}$$

where x_i is the mole fraction of component i in the liquid phase. The mole fraction is defined as:

$$x_i = \frac{\rho_i}{\sum_{i=1}^{Nc}\rho_i} \tag{8}$$

The influence parameter contains the information of the intermolecular geometry of the inhomogeneous fluid (interface) and relates the deviation of the Helmholtz energy density and the chemical potential in the interface due to the density gradient. This energy deviation ultimately manifests itself in a contribution of the density gradient to the interfacial tension [14,15,32,35–38]. Due to the generality of the linear gradient theory, this parameter is treated as a purely empirical parameter dependent with temperature.

The mixture influence parameter is comprised of the pure component influence parameter, c_{ii}, and the crossed influence parameter c_{ij}. The crossed influence parameter is determined via the binary interaction coefficient, l_{ij}, and Eq. [9].

$$c_{ij} = \sqrt{c_{ii}c_{jj}}(1 - l_{ij}) \tag{9}$$

In this work, both the SRK EoS and the PR EoS were used as the base equations of state in the linear gradient theory. The generalized form of these two equations is shown in Eq. (10).

$$P = \frac{RT}{v-b} - \frac{a(T)}{(v+\delta_1 b)(v+\delta_2 b)} \tag{10}$$

where the constants are $\delta_1 = 1$ and $\delta_2 = 0$ for the SRK EoS and $\delta_1 = 1+\sqrt{2}$ and $\delta_2 = 1-\sqrt{2}$ for the PR EoS. In Eq. (10) R is the universal gas constant, a the "attraction" constant, b the "repulsive" constant and v is the molar volume. With the thermodynamic definitions that can be found in Michelsen and Mollerup [39], the chosen equation of state can be transformed into an expression for the Helmholtz energy and the chemical potential. The mixture Helmholtz energy density, $f^0(\rho)$, is obtained from:

$$f^0(\rho) = \frac{A(T,V,\vec{n})}{V} = \frac{A^*(T,V,\vec{n})}{V} + \frac{A^{RES}(T,V,\vec{n})}{V} \tag{11}$$

The ideal portion of the Helmholtz energy, $A^*(T,V,\vec{n})$, is a sum of the contributions of the pure components in their ideal gas state:

$$A^*(T,V,\vec{n}) = \sum_{i}^{Nc} n_i A_i^*(T,V,n_i) \tag{12}$$

where the pure ideal gas Helmholtz energy is:

$$A_i^*(T,V,n_i) = -PV + n_i\mu_i^*(T,P) \tag{13}$$

In the above equations, V is the total volume, n is the number of moles and n_i is the number of moles of component i. Considering the equation of state for a pure component in the ideal gas state, $PV = n_iRT$, Eq. (13) becomes:

$$A_i^*(T,V,n_i) = -n_iRT + n_i\mu_i^*(T,P) \tag{14}$$

The chemical potential, or Gibbs energy, of the pure component i depends on the reference pressure. The isothermal change of the Gibbs energy, $d\mu = -SdT + VdP$, (where S is the entropy) of a pure ideal gas component leads to:

$$\mu_i^*(T,P) = \mu_i^*(T,P^{REF}) + RT\ln\left(\frac{P}{P^{REF}}\right) \tag{15}$$

Eq. (15) combined with Eq. (14) leads to:

$$A_i^*(T,V,n_i) = -n_iRT + n_i\left[\mu_i^*(T,P^{REF}) + RT\ln\left(\frac{P}{P^{REF}}\right)\right] \tag{16}$$

Substitution of the ideal gas equation of state into Eq. (16) gives:

$$A_i^*(T,V,n_i) = -n_iRT + n_i\left[\mu_i^*(T,P^{REF}) + RT\ln\left(\frac{n_iRT}{P^{REF}V}\right)\right] \tag{17}$$

Substitution into Eq. (12) gives the Helmholtz energy of an ideal gas mixture:

$$A^*(T,V,\vec{n}) = \sum_{i}^{Nc} n_i\left[-RT + \mu_i^*(T,P^{REF}) + RT\ln\left(\frac{n_iRT}{P^{REF}V}\right)\right] \tag{18}$$

or

$$\frac{A^*(T,V,\vec{n})}{V} = \sum_{i}^{Nc}\rho_i\left[-RT + \mu_i^*(T,P^{REF}) + RT\ln\left(\frac{\rho_iRT}{P^{REF}}\right)\right] \tag{19}$$

where $\rho = n/V$ and $\rho_i = n_i/V$. The residual term of the Helmholtz energy is obtained directly from the generalized cubic EoS [39]:

$$A^{RES}(T,V,\vec{n}) = -\int_{\infty}^{V}\left(P - \frac{nRT}{V}\right)dV \tag{20}$$

to give:

$$\frac{A^{RES}(T,V,\vec{n})}{V} = -\rho RT\ln(1-\rho b) - \frac{\rho a}{b(\delta_1-\delta_2)}\times\ln\left[\frac{1+\delta_1\rho b}{1+\delta_2\rho b}\right] \tag{21}$$

The addition of the ideal and the residual Helmholtz energies results in the overall Helmholtz energy density:

$$f^0(\rho) = \sum_i^{Nc} \rho_i \mu_i^*(T, P^{REF}) + RT \sum_i^{Nc} \rho_i \ln\left(\frac{\rho_i RT}{P^{REF}}\right) - \rho RT - \rho RT \ln(1-\rho b) - \frac{\rho a}{b(\delta_1-\delta_2)} \ln\left[\frac{1+\delta_1\rho b}{1+\delta_2\rho b}\right] \quad (22)$$

The chemical potential is obtained from the derivative of the Helmholtz energy density with respect to the molar density of component i:

$$\mu_i(T, V, \vec{n}) = \left(\frac{\partial A(T, V, \vec{n})}{\partial n_i}\right)_{T,V,n_j} = \left(\frac{\partial A^*(T, V, \vec{n})}{\partial n_i}\right)_{T,V,n_j} + \left(\frac{\partial A^{RES}(T, V, \vec{n})}{\partial n_i}\right)_{T,V,n_j} \quad (23)$$

$$\left(\frac{\partial A^*(T, V, \vec{n})}{\partial n_i}\right)_{T,V,n_j} = \mu_i^*(T, P^{REF}) + RT \ln\left(\frac{\rho_i RT}{P^{REF}}\right) \quad (24)$$

$$\left(\frac{\partial A^{RES}(T, V, \vec{n})}{\partial n_i}\right)_{T,V,n_j} = -\frac{2\sum_j^{Nc} \rho_j a_{ij}}{\rho b(\delta_1-\delta_2)} \ln\left[\frac{1+\delta_1\rho b}{1+\delta_2\rho b}\right] + \frac{ab_i}{b^2(\delta_1-\delta_2)} \times \ln\left[\frac{1+\delta_1\rho b}{1+\delta_2\rho b}\right] + \frac{\rho RTb_i}{(1-\rho b)} - \frac{\rho b_i a}{b(1+\delta_1\rho b)(1+\delta_2\rho b)} - RT\ln(1-\rho b) \quad (25)$$

which results in Eq. (26), the chemical potential of component i.

$$\mu_i(T, V, \vec{n}) = \mu_i^*(T, P^{REF}) + RT \ln\left(\frac{\rho_i RT}{P^{REF}}\right) - \frac{2\sum_j^{Nc} \rho_j a_{ij}}{\rho b(\delta_1-\delta_2)} \ln\left[\frac{1+\delta_1\rho b}{1+\delta_2\rho b}\right] - RT\ln(1-\rho b) + \frac{ab_i}{b^2(\delta_1-\delta_2)} \ln\left[\frac{1+\delta_1\rho b}{1+\delta_2\rho b}\right] + \frac{\rho RTb_i}{(1-\rho b)} - \frac{\rho b_i a}{b(1+\delta_1\rho b)(1+\delta_2\rho b)} \quad (26)$$

The linear gradient theory (and gradient theory) modelling approach requires an equation of state for the determination of the phase behaviour of the bulk homogenous phases and the homogenous phases at the required compositions in the inhomogeneous phase as determined by the linear distribution of the composition in the interface. At each temperature and pressure of interest, the compositions and densities of the homogenous phases were determined with an isothermal flash routine similar to the flash algorithm presented in Michelsen and Mollerup [39] and Whitson and Brulé [40].

After the interface was broken down into an arbitrary number of points, and the composition distributed linearly, the chemical potential of each species, Eq. (26), Helmholtz energy, Eq. (22), and grand thermodynamic potential energy, Eq. (5), at each point (including the bulk homogenous phases) were determined. The influence parameter of the mixture was then determined with the pure component influence parameters and the mixing rule in Eq. (6). Finally the interfacial tension calculation, Eq. (3), was determined via numerical integration. A more detailed calculation procedure is presented in [3].

The phase behaviour of the methane–water system was determined at each temperature and pressure of interest using the flash calculation procedure. The a and b (pure and mixture) parameters were determined from the critical constants and acentric factors from the compilation of Rowley et al. [41]. The binary interaction parameter, k_{12}, which appears in the mixing rule of the equations of state, was set to zero.

4. Pure methane and water influence parameters

The pure component influence parameters, c_{ii}, of both methane and water were determined from the minimization of the calculated interfacial tension and those presented in Vargarftik et al. [42]. The gradient theory combined with classical equations of state has been shown [14–16] to incorrectly reproduce the interfacial tensions of fluid systems at reduced temperatures greater than approximately 0.9. As such, only pure component interfacial tensions at reduced temperatures less than 0.9 were used to obtain the pure component influence parameters. The results for the SRK and PR equations of state are presented in Eqs. (27)–(30) as the dimensionless ratio $c/ab^{2/3}$.

Expressions similar to Zuo and Stenby [3] were used to correlate the influence parameters of both methane and water. The influence parameter of water is presented in Eqs. (27) and (28):

$$\text{SRK EoS}: \quad \frac{c_{11}}{a_{11}b_{11}^{2/3}} = -4.9109\times10^{-1} + 4.7426\times10^{-3}T - 1.2320\times10^{-5}T^2 + 1.3238\times10^{-8}T^3 \quad (27)$$

$$\text{PR EoS}: \quad \frac{c_{11}}{a_{11}b_{11}^{2/3}} = -2.9499\times10^{-1} + 2.9449\times10^{-3}T - 7.3898\times10^{-6}T^2 + 7.9495\times10^{-9}T^3 \quad (28)$$

And the influence parameter of methane is presented in Eqs. (29) and (30):

$$\text{SRK EoS}: \quad \frac{c_{22}}{a_{22}b_{22}^{2/3}} = 0.3587\left(1-\frac{T}{T_c}\right)^{-0.4977} \quad (29)$$

$$\text{PR EoS}: \quad \frac{c_{22}}{a_{22}b_{22}^{2/3}} = 0.2852\left(1-\frac{T}{T_c}\right)^{-0.4299} \quad (30)$$

Methane was always supercritical at all of the conditions in the collected data set. Zuo and Stenby [19] suggested setting the reduced temperature of the supercritical component to single value. In this investigation the influence parameter of methane, c_{22}, was set to a constant value, which is obtained from Eqs. (29) or (30) at a reduced temperature of 0.5. The influence parameter for water was obtained from Eqs. (27) and (28) at all the temperatures studied.

5. Mixture influence parameter and results

After a robust examination of the all the collected data, the data set of Hocott was not considered in this investigation. The data of Hocott was rejected due to the fact that a gas mixture of methane with small amounts of ethane and propane and a subsurface sample of water were used instead of pure methane or water. The higher temperature data of Hough et al., temperatures greater than 296.4 K (310.9, 344.3, 377.6 and 410.9 K), were not used in the linear gradient parameter determination. The higher temperature data of Hough et al. were not used because of the data's inconsistency with the rest of the data set and the results obtained from the model.

Preliminary screening of the data consisted of fitting the binary interaction coefficient for the mixture influence parameter to all the data and any data (isotherms) which significantly deviated from the overall absolute average percent deviation (AAPD) were discarded and a new regression of the parameters was performed. Interfacial tensions on an individual basis were not screened. Screening only the isotherms appeared to be a good basis on which to evaluate and screen the collected data set. The objective function used in this investigation was that of Weiland et al. [43,44]:

$$\text{obj} = \sum_{i=1}^{\text{NP}} \left(\frac{\left[\gamma^{\text{calc}} - \gamma^{\text{exp}}\right]^2}{\gamma^{\text{calc}}\gamma^{\text{exp}}} \right)_i \tag{31}$$

which weights all of the number of data points, NP, (high and low interfacial tensions) equally.

The previous correlation investigations by Argaud [6], Firoozabadi and Ramey [7,5] Zuo and Stenby [3] and Yan et al. [22] (Zhao et al. [23]) did not use the data of Hocott and Hough et al. in their model development. Firoozabadi and Ramey only used the data of Jennings and Newman in their model development. Argaud and Zuo and Stenby only considered the data of Jennings and Newman and Jho and King and Yan et al. only considered the data of Sachs and Meyn.

Although recommended in the previous modelling applications of Argaud, Firoozabadi and Ramey and Zuo and Stenby, the higher temperature data of Jennings and Newman appeared to exhibit a strong discrepancy with the rest of the data set and the results obtained from the model. In fact the isotherms of 373.2 and 449.8 K produced the largest AAPD (4–5 times the overall AAPD) when compared to the results of the models. Based on these preliminary results the 373.2 and 449.8 K isotherms of Jennings and Newman were not used in the final l_{12} parameterisation.

The remainder of the data set, ranging in temperature from 275.2 to 473 K and pressures up to 240.0 MPa was used to determine l_{12} found in Eq. (9). The binary interaction coefficient for the mixture influence parameter was found to be dependent on the temperature and the temperature dependence was best represented by the following equations:

$$\text{SRK EoS}: \quad l_{12} = 3.7700 \times 10^{-2} + 3.0775 \times 10^{-2} \times \exp\left(-\frac{T}{-1.3340 \times 10^2}\right) \tag{32}$$

$$\text{PR EoS}: \quad l_{12} = 7.4241 \times 10^{-2} + 2.0218 \times 10^{-2} \times \exp\left(-\frac{T}{-1.1171 \times 10^2}\right) \tag{33}$$

As can be seen in Table 2, these binary interaction coefficients for the mixture influence parameter reproduced the experimental data very well with an overall AAPD in the interfacial tension of 2.3% for the LGT-SRK and 2.5% for the LGT-PR, somewhat less than the estimated experimental uncertainty. The total number of points used to determine l_{12} was 236 compared to the 286 available in the database. It should be pointed out that the calculation of the interfacial tension is very sensitive with the influence parameter and hence l_{12}. The results in Table 2 indicate that the LGT modelling approach with the influence parameters and the binary interaction coefficient determined in this investigation reproduce the collected data very well. The model performs equally well over the almost 200 K temperature range with pressures up to 260 MPa. The results from the LGT-PR and LGT-SRK models are similar and as such only the results from the LGT-SRK model are presented in the following figures.

The 275.2 K interfacial tension–pressure isotherm is presented in Fig. 1. As can be seen the model somewhat over predicts the data of Jho et al. and this over prediction increases with increasing pressure. This trend is also exhibited at all the temperatures investigated by Jho et al.

Table 2
Absolute average percentage deviation of the calculated interfacial tension for the methane–water system

Investigators	NP	SRK-LGT AAPD (%)	PR-LGT AAPD (%)
Hough et al. [25]	5	1.7	1.9
Slowinski et al. [26]	5	3.9	4.1
Jennings and Newman [27]	11	1.7	1.7
Massoudi and King [28]	10	2.5	2.6
Jho et al. [29]	62	2.0	2.2
Wiegand and Franck [30]	23	2.8	3.4
Sachs and Meyn [9]	34	2.7	2.9
Tian et al. [31]	15	2.7	3.1
Ren et al. [33]	30	1.6	1.9
Zhao et al. [23]	35	2.5	2.8
Sun et al. [34]	6	1.1	1.4
Overall	236	2.3	2.5
Lepski [32]	30	3.1	2.7

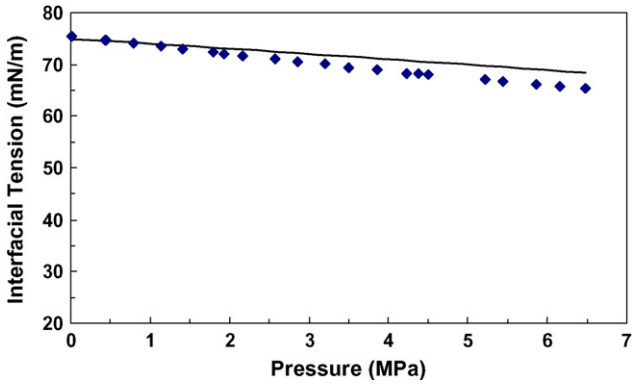

Fig. 1. Interfacial tension of the methane–water system at 275.2 K: closed diamonds, Jho et al. [29]; solid line, LGT-SRK.

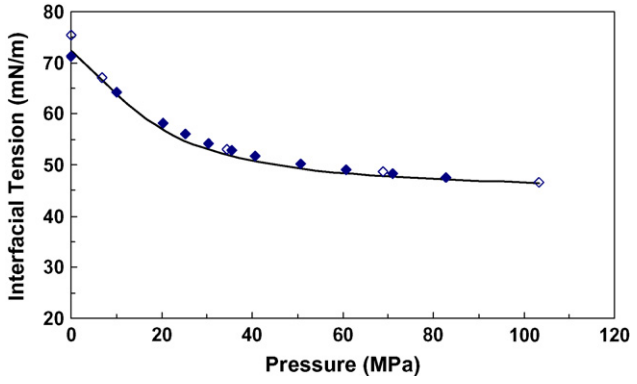

Fig. 2. Interfacial tension of the methane–water system at 296.5 K: closed diamonds, Hough et al. [25]; open diamonds, Jennings and Newman [27]; solid line, LGT-SRK.

Despite the discrepancies with the data sets at elevated temperatures, the data at 296.5 K of both Hough et al. and Jennings and Newman are quite well represented by the model as exhibited in Fig. 2. The experimental data at 298 K, shown in Fig. 3, are quite similar and the model represents the data of this isotherm

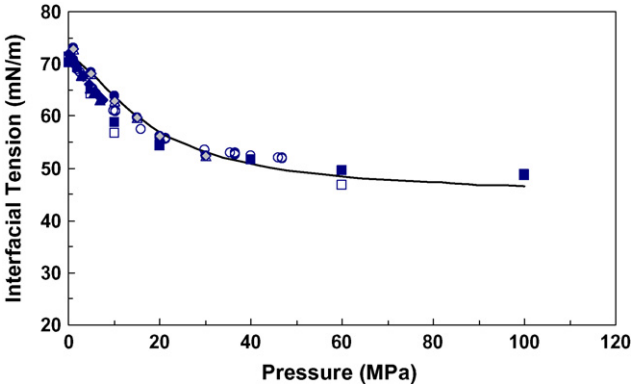

Fig. 3. Interfacial tension of the methane–water system at 298.2 K: closed diamonds, Jho et al. [29]; open diamonds, Massoudi and King [28]; closed circles, Ren et al. [33]; open circles, Sachs and Meyn [9]; closed triangles, Slowinski et al. [26]; open triangles, Sun et al. [34]; closed squares, Tian et al. [31] (298.0 K); open squares, Wiegand and Franck [30] (298.0 K); grey diamonds, Zhao et al. [23]; solid line, LGT-SRK.

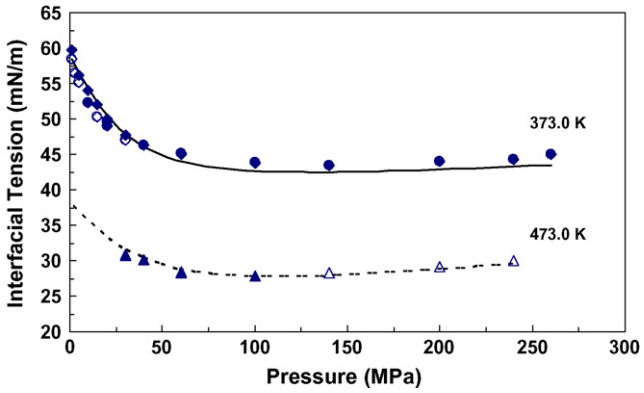

Fig. 4. Interfacial tension of the methane–water system at 373.2 K: closed diamonds, Ren et al. [33]; open diamonds, Tian et al. [31] (373.0 K); closed circles, Wiegand and Franck [30]; open circles, Zhao et al. [23] (373.0 K); solid line, LGT-SRK and 473.0 K: closed triangles, Tian et al. [31]; open triangles, Wiegand and Franck [30]; dashed line, LGT-SRK.

quite well. The majority of the low-pressure data is slightly overestimated at this temperature.

Fig. 4 illustrates the differences between the data from Jennings and Newman, Tian et al., Ren et al., Wiegand and Franck and Yan et al. at 373 K. The data from these investigations are more or less consistent with each other, even at high pressures. This figure also shows how the LGT model seems to correctly capture the slight increase in the experimentally determined interfacial tensions at both 373 and 473 K by Wiegand and Franck.

Unfortunately, only Wiegand and Franck investigated this system at pressures which exhibited a minimum in interfacial tension with increasing pressure. This minimum has been seen in other hydrocarbon–water systems [30,45] were the LGT is presently being used to correlate the other relevant hydrocarbon–water systems. This increase in methane–water interfacial tension at high temperatures and pressures may be explained by recent Molecular Dynamics Simulations [46–49] which have shown that at increased temperatures, the reduction of the hydrogen bonds results in (1) increased mutual penetration of methane and water, (2) a stronger "roughening" of the surface and even periodic "throwing" of water clusters into the methane rich phase. Both of these effects become more pronounced at higher pressures.

After the binary interaction determination, the additional dataset of Lepski was discovered and these data, which were not used in the l_{12} parameterisation, were used as an a posteriori check of the LGT model and the parameters obtained in this investigation. The data from Lepski consisted of an additional 30 interfacial tension data points ranging in temperature from 325.6 to 400 K and pressures from 10.3 to 24.1 MPa. Overall, the models were successfully able to calculate this data to within an AAPD of 3.2% for the LGT-SRK model and 2.7% for the LGT-PR model. The model results and the experimental data are presented in Fig. 5. These results support the success of the modelling approaches and show that the dataset of Lepski are of a quality consistent to those used in the parameterisation.

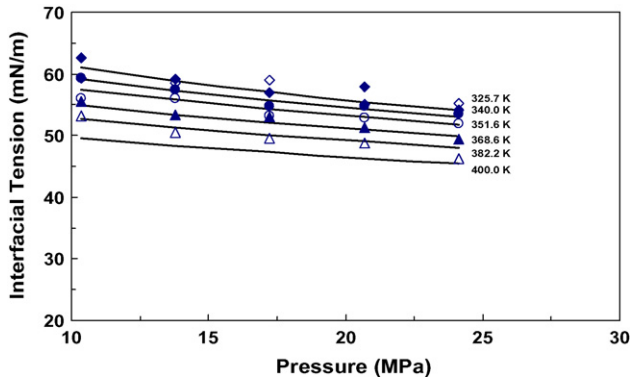

Fig. 5. Interfacial tension of the methane–water system data of Lepski [32]: closed diamonds, 325.7 K; open diamonds, 340.0 K; closed circles, 351.6 K; open circles, 368.6 K; closed triangles, 382.2 K; open triangles, 400.0 K; solid line, LGT-SRK.

6. Conclusions

An exhaustive literature survey to obtain all the binary methane–water interfacial tension data available in the open literature was performed. All the published data were reviewed and the LGT combined with the Soave–Redlich–Kwong and the Peng–Robinson equations of state was successfully applied to obtain the necessary pure component influence parameters and the binary interaction coefficient for the mixture influence parameter. The literature review and the application of the LGT identified large discrepancies in the data sets when compared to the modelling results and the existing data sets.

The evaluation of the collected data and the regression of the necessary parameters in the LGT combine to provide excellent results when tested against the collected data set. When tested against an additional data set, found later on in the investigation, the calculations from the LGT and the new parameters were very satisfactory. The results obtained here illustrate that the LGT model with the new parameters provides a simple and accurate technique to calculate the interfacial tension of the methane–water system over a large temperature and pressure range.

References

[1] S.J. O'Connor, AAPG Bull. 84 (2000) 1537–1541.
[2] R. Amin, T.N. Smith, Fluid Phase Equilib. 142 (1998) 231–241.
[3] Y.X. Zuo, E.H. Stenby, In Situ 22 (1998) 157–180.
[4] E.J. Mackay, G.D. Henderson, D.H. Tehrani, A. Danesh, SPE Reserv. Eval. Eng. 1 (1998) 408–415.
[5] A. Firoozabadi, H.J. Ramey Jr., J. Can. Petrol. Technol. 27 (1988) 41–48.
[6] M.J. Argaud, Proceedings of the 3rd Society of Core Analysts European Core Analysis Symposium: Advances in Core Evaluation III. Reservoir Management, 1993, pp. 147–174.
[7] A. Firoozabadi, H.J. Ramey Jr., Preprints of the 38th Annual CIM Petroleum Society Technical Meeting, vol. 2, 1987, pp. 533–554.
[8] B. Lepski, Z. Bassiouni, J.M. Wolcott, SPE 39659, Paper Presented at the SPE/DOE Improved Oil Recovery Symposium, Oklahoma, U.S.A., April 19–22, 1998, pp. 61–71.
[9] W. Sachs, V. Meyn, Colloids Surf. A 94 (1995) 291–301.
[10] W. Sachs, V. Meyn, Erdoel Erdgas Kohle 111 (1995) 119–121.
[11] Y.X. Zuo, E.H. Stenby, Can. J. Chem. Eng. 75 (1997) 1130–1137.
[12] D.S. Schechter, B. Guo, SPE Reserv. Eval. Eng. 1 (1998) 207–217.
[13] D. Broseta, K. Ragil, SPE 30784, Paper Presented at the SPE Annual Technical Conference and Exhibition, Dallas, Texas, U.S.A., October, 1995, pp. 22–25.
[14] B.S. Carey, The Gradient Theory of Fluid Interfaces, Ph.D. Dissertation, University of Minnesota, Minnesota, U.S.A., 1979.
[15] P.M.W. Cornelisse, The Square Gradient Theory Applied: Simultaneous Modelling of Interfacial Tension and Phase Behaviour, Ph.D. Dissertation, Technische Universiteit Delft, Delft, The Netherlands, 1997.
[16] C. Miqueu, Modélisation á Température et Pression Elevées de la Tension Superficielle de Composants des Fluides Pétroliers et de Leurs Mélanges Synthétiques ou Réels, Ph.D. Dissertation, Université de Pau, Pau, France, 2001.
[17] Y.X. Zuo, E.H. Stenby, J. Colloid Interface Sci. 182 (1996) 126–132.
[18] Y.X. Zuo, E.H. Stenby, J. Chem. Eng. Jpn. 29 (1996) 159–165.
[19] Y.X. Zuo, E.H. Stenby, SPE J. 3 (1998) 134–145.
[20] D.Y. Peng, D.B. Robinson, Ind. Eng. Chem. Fund. 15 (1976) 59–64.
[21] G. Soave, Chem. Eng. Sci. 27 (1972) 1197–1203.
[22] W. Yan, G.Y. Zhao, G.J. Chen, T.M. Guo, J. Chem. Eng. Data 46 (2001) 1544–1548.
[23] G. Zhao, W. Yan, G. Chen, X. Guo, Shiyou Daxue Xuebao, Ziran Kexueban 26 (2002) 75–78.
[24] C.R. Hocott, Transactions of the American Institute of Mining, Metallurgical Engineers, Petrol. Dev. Technol. 132 (1939) 184–191.
[25] E.W. Hough, M.J. Rzasa, B.B. Wood, J. Petrol. Technol. 3 (1951) 57–60.
[26] E.J. Slowinski Jr., E.E. Gates, C.E. Waring, J. Phys. Chem. 61 (1957) 808–810.
[27] H.Y. Jennings Jr., G.H. Newman, Soc. Petrol. Eng. J. 11 (1971) 171–175.
[28] R. Massoudi, A.D. King Jr., J. Phys. Chem. 79 (1975) 1670–1675.
[29] C. Jho, D. Nealon, S. Shogbola, A.D. King Jr., J. Colloid Interface Sci. 65 (1978) 141–154.
[30] G. Wiegand, E.U. Franck, Bunsen Phys. Chem. 98 (1994) 809–817.
[31] Y. Tian, Y. Xiao, H. Zhu, X. Dong, X. Ren, F. Zhang, Wuli Huaxue Xuebao 13 (1997) 89–95.
[32] B. Lepski, Gravity Assisted Tertiary Gas Injection Process in Water Drive Oil Reservoirs, Ph.D. Dissertation, Louisiana State University and Agricultural & Mechanical College, Louisiana, U.S.A., 1997.
[33] Q.Y. Ren, G.J. Chen, W. Yan, T.M. Guo, J. Chem. Eng. Data 45 (2000) 610–612.
[34] C.Y. Sun, G.J. Chen, L.Y. Yang, J. Chem. Eng. Data 49 (2004) 1023–1025.
[35] Y.X. Zuo, E.H. Stenby, Fluid Phase Equilib. 132 (1997) 139–158.
[36] H.T. Davis, L.E. Scriven, Adv. Chem. Phys. 49 (1982) 357–454.
[37] V. Bongiorno, L.E. Scriven, H.T. Davis, J. Colloid Interface Sci. 57 (1976) 462–475.
[38] H.T. Davis, L.E. Scriven, SPE 9278, Paper Presented at the 55th Annual Fall Technical Conference and Exhibition of the Society of Petroleum Engineers of AIME, Dallas, U.S.A., September 21–24, 1980.
[39] M.L. Michelsen, J.M. Mollerup, Thermodynamic Models, Fundamentals and Computational Aspects, Tie-Line Publications, Holte, Denmark, 2004.
[40] C.H. Whitson, M.R. Brulé, Phase Behavior, Society of Petroleum Engineers Inc., Richardson, Texas, U.S.A., 2000.
[41] R.L. Rowley, W.V. Wilding, J.L. Oscarson, Y. Yang, N.A. Zundel, T.E. Daubert, R.P. Danner, DIPPR Data Compilation of Pure Compound Properties, Design Institute for Physical Properties, American Institute of Chemical Engineers, New York, U.S.A., 2005.
[42] N.B. Vargaftik, Y.K. Vinogradov, V.S. Yargin, Handbook of Physical Properties of Liquids and Gases—Pure Substances and Mixtures, third ed., Begall House Inc., New York, U.S.A., 1996.
[43] R.H. Weiland, T. Chakravarty, A.E. Mather, Ind. Eng. Chem. Res. 32 (1993) 1419–1430.
[44] R.H. Weiland, T. Chakravarty, A.E. Mather, Ind. Eng. Chem. Res. 34 (1995) 3173.
[45] H.Y. Jennings Jr., J. Colloid Interface Sci. 24 (1967) 323–329.
[46] B. Kvamme, T. Kuznetsova, K.A.G. Schmidt, WSEAS Trans. Biol. Biomed. 3 (2006) 517–523.
[47] B. Kvamme, T. Kuznetsova, K.A.G. Schmidt, Lecture Series on Computer and Computational Sciences, vol. 7, VSP International Science Publishers, 2006, pp. 284–287.

[48] B. Kvamme, T. Kuznetsova, K.A.G. Schmidt, Molecular Dynamics Simulations and Numerical Modelling of Interfacial Tension in Water-Methane Systems, Presentation at the 4th WSEAS International Conference on Heat and Mass Transfer, Gold Coast, Australia, January, 17–19, 2007.

[49] B. Kvamme, T. Kuznetsova, K.A.G. Schmidt, Experimental Measurements and Numerical Modelling of Interfacial Tension in Water-Methane Systems, Presentation at the International Conference of Computational Methods in Sciences and Engineering, Chania, Greece, October 27-November 1, 2006.